

**Supplementary Materials for “Structurally decoupled stiffness and solute transport in multi-arm poly(ethylene glycol) hydrogels”**

Nathan R. Richbourg<sup>1</sup> & Nicholas A. Peppas<sup>1-4</sup>

<sup>1</sup>Department of Biomedical Engineering, University of Texas, Austin, TX 78712, USA.

<sup>2</sup>McKetta Department of Chemical Engineering, University of Texas, Austin, TX 78712, USA.

<sup>3</sup>Division of Molecular Therapeutics and Drug Delivery, College of Pharmacy, University of Texas, Austin, TX 78712, USA.

<sup>4</sup>Departments of Surgery and Pediatrics, Dell Medical School, University of Texas, Austin, TX 78712, USA.

\*Corresponding Author Contact: [nrichbourg@utexas.edu](mailto:nrichbourg@utexas.edu)

**Links to raw datasets, R scripts, and GraphPad Files on Figshare.com:**

Entire collection:

<https://doi.org/10.6084/m9.figshare.c.6425846.v2>

Raw datasets:

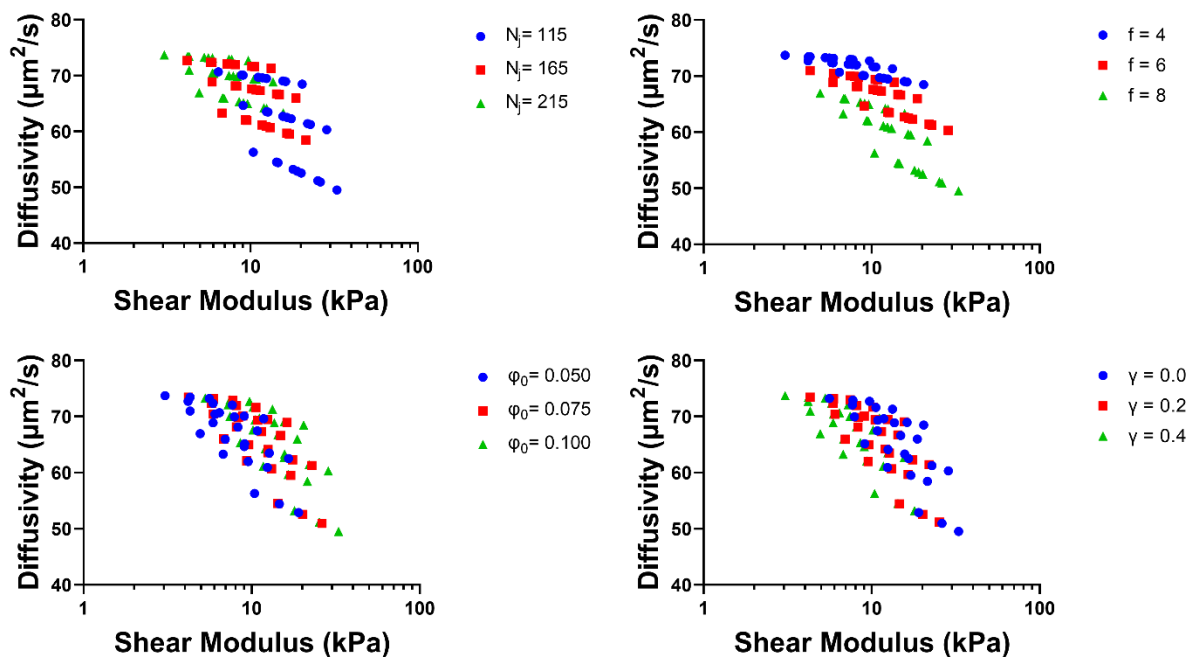
<https://doi.org/10.6084/m9.figshare.22012889.v1>

R Script:

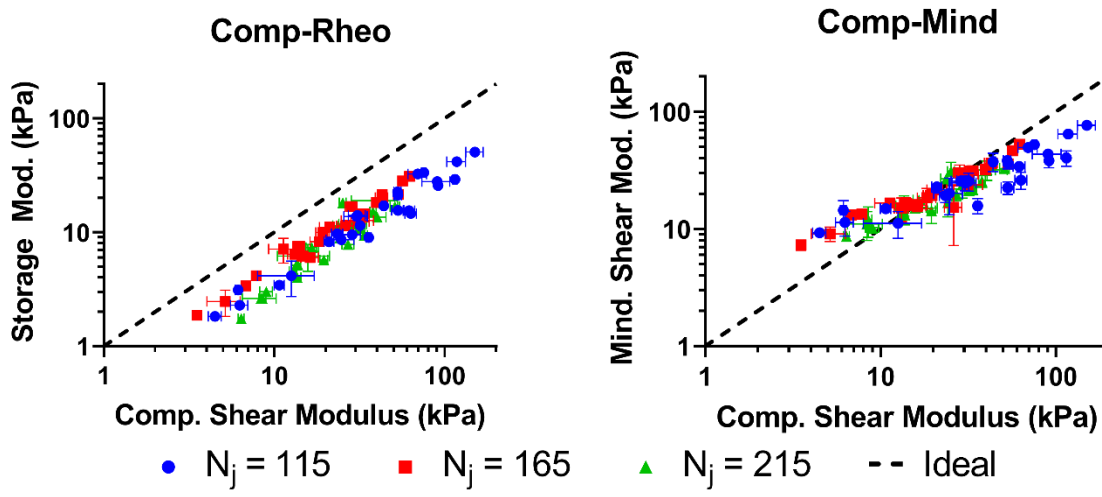
<https://doi.org/10.6084/m9.figshare.22083539.v1>

GraphPad Prism Files:

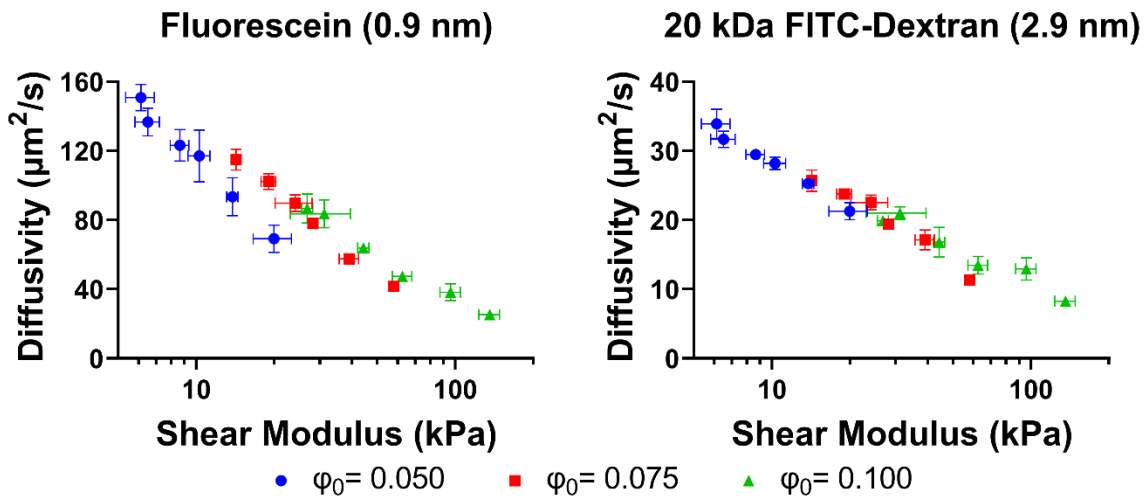
<https://doi.org/10.6084/m9.figshare.23818425.v1>



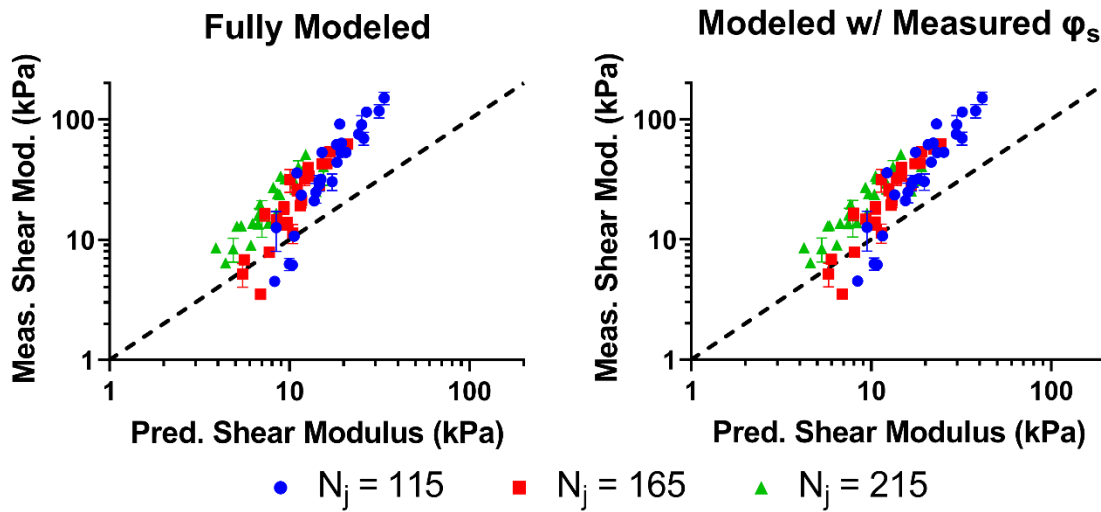
**Supplementary Figure S1. Swollen Polymer Network Model predictions of structural parameter influences on the shear modulus and diffusivity of 20 kDa FITC-dextran in multi-arm PEG hydrogels.** Degree of polymerization between junctions ( $N_j$ ), initial polymer volume fraction ( $\phi_0$ ), junction functionality ( $f$ ), and frequency of chain-end defects ( $\gamma$ ).



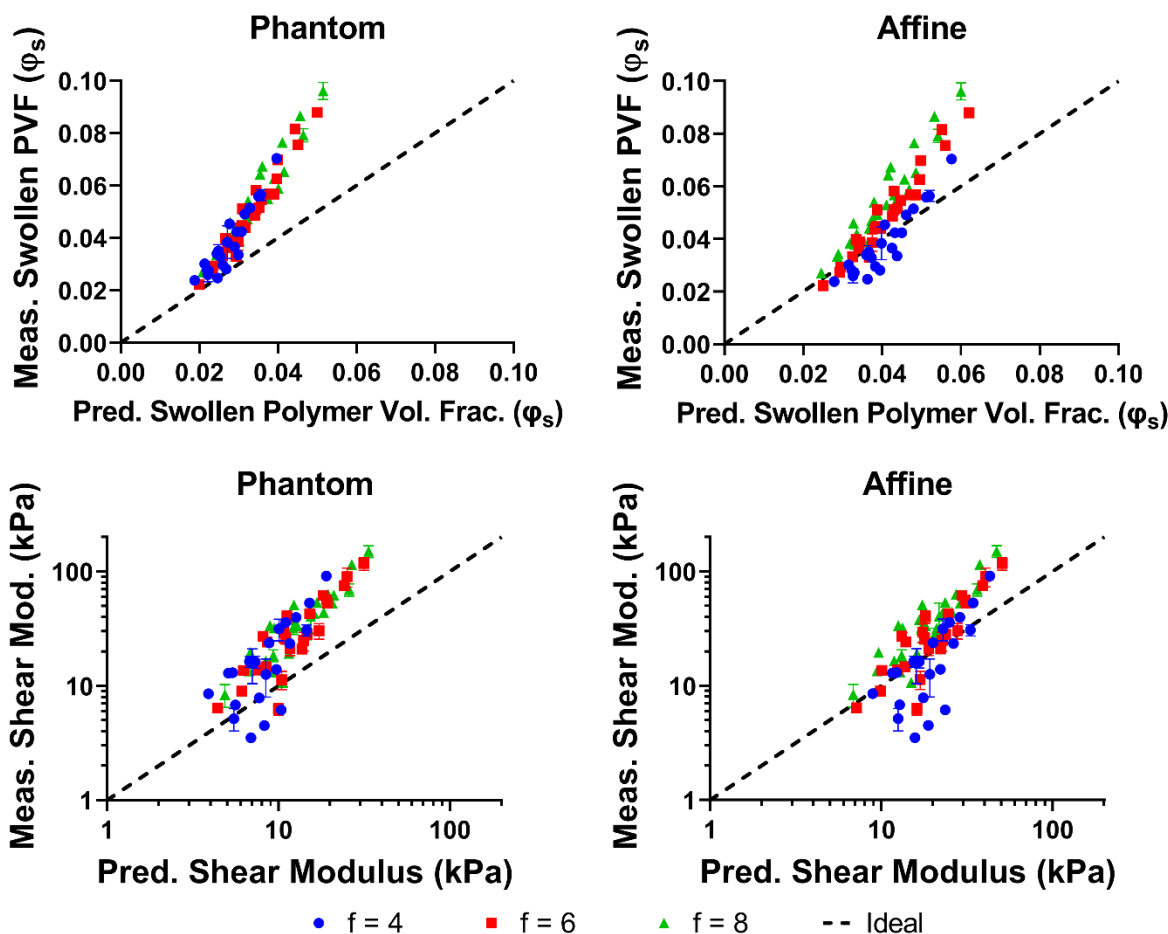
**Supplementary Figure S2. Comparative stiffness of multi-arm PEG hydrogels via compression, rheology, and macroindentation.** Compressive shear moduli are consistently higher than rheological storage moduli (A) but cross over from higher to lower than macroindentation shear moduli (B). Error bars represent standard deviations ( $n = 3$ ).



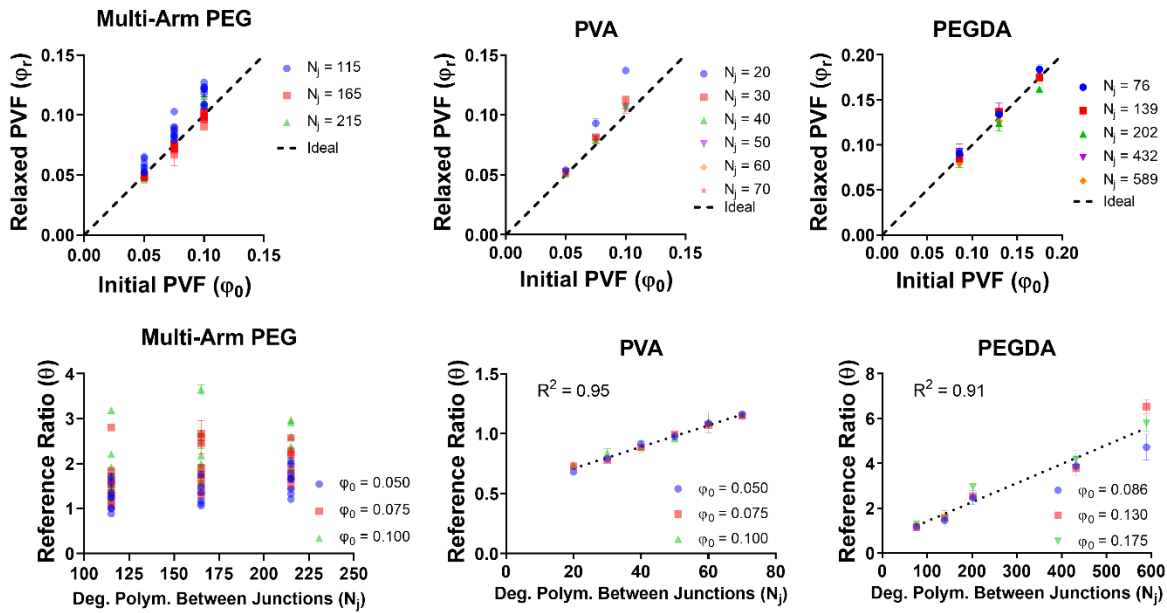
**Supplementary Figure S3. Correlation between shear modulus and solute diffusivity in poly(vinyl alcohol) hydrogel formulations with variations in the initial polymer volume fraction ( $\phi_0$ ) and degree of polymerization between junctions ( $N_j = 20, 30, 40, 50, 60, 70$ ).** Data were taken from our previous publications, Refs.[44, 47] Increasing the degree of polymerization between junctions increased solute diffusivity and decreased shear modulus.



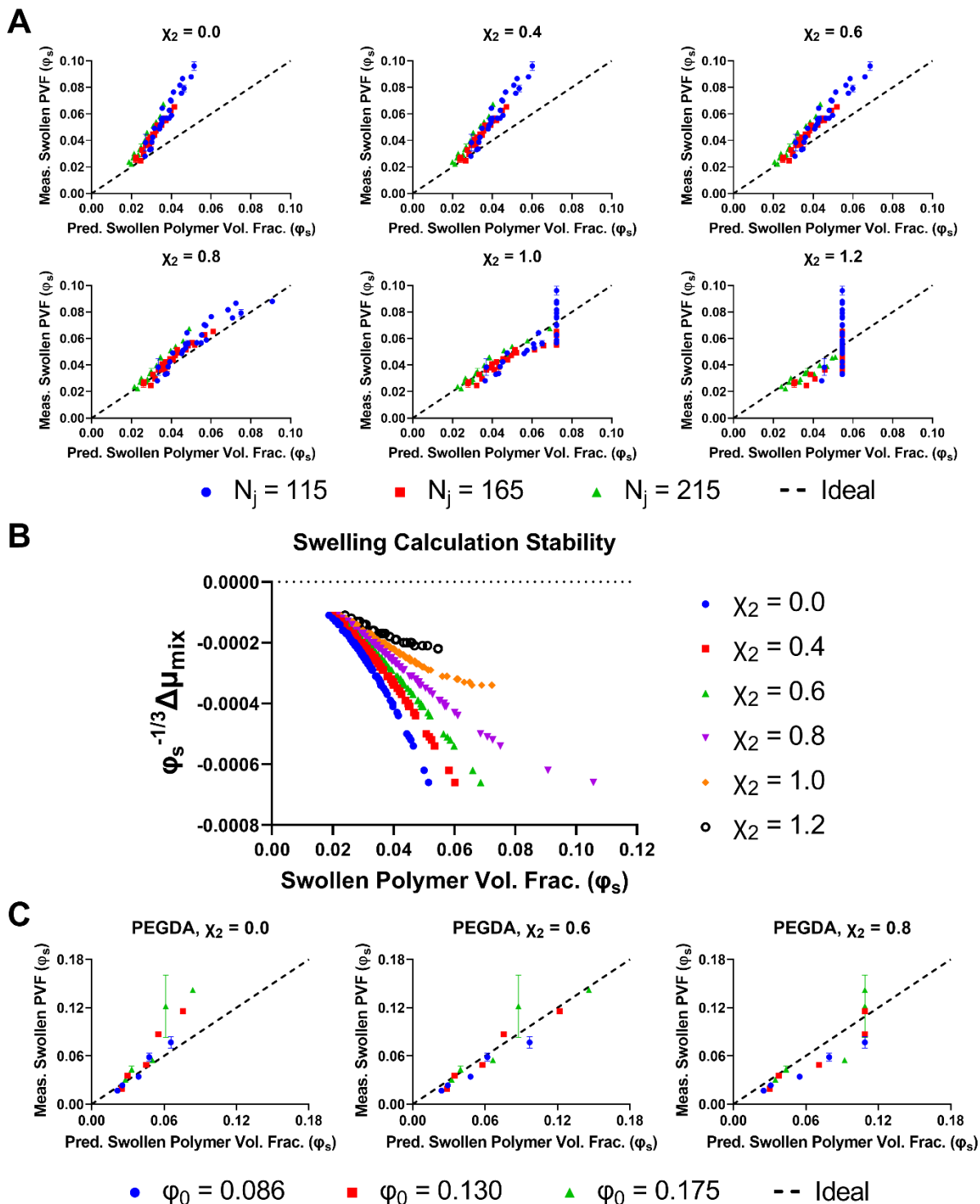
Supplementary Figure S4. Using the measured swollen polymer volume fraction ( $\phi_s$ ) when predicting shear modulus minimally improves the prediction-measurement correlation.



**Supplementary Figure S5. Comparing phantom and affine model effects on predicted swollen polymer volume fraction and shear modulus.** The phantom model prediction shows an accurate relationship between junction functionality and swelling as well as junction functionality and shear stiffness, unlike the affine model. Error bars represent standard deviations ( $n = 3$ ).



**Supplementary Figure S6. Multi-arm PEG hydrogels do not match the precise swelling relationships previously observed for PVA hydrogels and PEGDA hydrogels.** While this may be partially a result of the additional structural parameters investigated, even changing the initial polymer volume fraction ( $\phi_0$ ) in multi-arm PEG hydrogels changed the reference ratio, directly contrasting the overlap for PVA and PEGDA hydrogels. Swelling measurement methods were consistent across hydrogel systems. PVA and PEGDA graphs adapted from our previous work.[42]



**Supplementary Figure S7. Evaluating  $\chi_2$  for PEG-based hydrogels.** (A) Increasing  $\chi_2$  up to 0.8 improves the correlation between predicted and measured swelling in multi-arm PEG hydrogels, but further increases create an artificial upper limit. (B) Analysis of the calculation stability shows divergent behavior at high  $\chi_2$  values consistent with the overall  $\chi$  exceeding 0.5.



(C) Analysis of previous swelling data in PEGDA hydrogels[42] shows improvement up to  $\chi_2 = 0$ .